JOURNAL OF BONE AND MINERAL RESEARCH
Volume 24, Number 8, 2009
Published online on March 16, 2009; doi: 10.1359/JBMR.090306

1α,25(OH)$_2$ Vitamin D$_3$ Induction of ATP Secretion in Osteoblasts

Payal Biswas and Laura P. Zanello

ABSTRACT: In the absence of mechanical stimulation, brief exposure of osteoblasts to 1α,25(OH)$_2$vitamin D$_3$ (1,25D) triggers plasma membrane electrical responses that couple to exocytosis. Here we describe for the first time 1,25D induction of exocytotic ATP release in static ROS 17/2.8 and SAOS-2 cells and primary calvarial osteoblasts expressing a vitamin D receptor (VDR). We found that 10 nM 1,25D optimally induced 45 ± 1% and 40 ± 1% of partial and complete exocytotic events, respectively, from a 1,25D-sensitive pool of ATP-containing secretory vesicles within 60 s. We measured a dose-dependent 1,25D induction of ATP secretion, with maximal response of ~6.2-fold (16.93 ± 1.82 nM for SAOS-2) and 3.1-fold (18.89 ± 1.39 nM for ROS 17/2.8) obtained with 10 nM 1,25D compared with basal ATP levels (2.75 ± 0.39 nM, SAOS-2; 6.09 ± 0.58 nM, ROS 17/2.8 cells). The natural metabolite 25(OH)vitamin D$_3$ (25D, 10 nM) induced a significant 3.6-fold increase of ATP release in ROS 17/2.8 cells, but there was no induction with the antagonist 1β,25(OH)$_2$vitamin D$_3$ (1β,25D, 10 nM) or the steroid 17β-estradiol (10 nM). 1,25D-induced ATP secretion was abolished when cells were preincubated with inhibitors of vesicular exocytosis. siRNA VDR silencing prevented 1,25D stimulation of ATP exocytosis in ROS 17/2.8 and SAOS-2 cells. Similarly, 1,25D failed to stimulate ATP exocytosis in primary osteoblasts from a VDR knockout mouse. ATP secretion coupled to 1,25D induction of cytosolic calcium and chloride channel potentiation. Rapid 1,25D stimulation of ATP secretion involving nontranscriptional VDR functions in osteoblasts may help explain 1,25D bone anabolic properties.
J Bone Miner Res 2009;24:1450–1460. Published online on March 16, 2009; doi: 10.1359/JBMR.090306

Key words: 1α,25(OH)$_2$vitamin D$_3$, ATP release, exocytosis, extranuclear vitamin D receptor, osteoblast

Address correspondence to: *Laura P. Zanello, PhD, Department of Biochemistry, University of California, 5436 Boyce Hall, Riverside, CA 92521, USA, E-mail: laura.zanello@ucr.edu*

INTRODUCTION

OSTEOBLASTS, THE BONE-FORMING cells, are a main target for calcitropic hormones including the steroid 1α,25(OH)$_2$-dihydroxyvitamin D$_3$ (1,25D). 1,25D direct effects on osteoblasts occur because of binding to and activation of the vitamin D receptor (VDR), which triggers a variety of nuclear and extranuclear cellular responses ultimately related to the production and maintenance of the adult skeleton.[1] On one hand, 1,25D/VDR functions as a transcription factor for the regulation of the expression of genes involved in osteoblast differentiation and bone matrix formation.[2] On the other hand, VDR activation initiates rapid (seconds to minutes), nongenotropic actions that include modulation of the electrical state of the osteoblast membrane, elevation of cytoplasmic calcium, and activation of protein kinases.[3–7] We showed previously that 1,25D nongenotropic actions at the plasma membrane level lead to ion channel activation[8,9] and induction of a regulated type of exocytosis in osteoblasts,[10,11] possibly related to bone anabolic functions of the hormone.

In osteoblasts, 1,25D increases intracellular calcium concentration by opening calcium-permeating channels present in the plasma membrane[12,13] and depleting internal Ca^{2+} stores.[6,14] 1,25D-promoted calcium signals have been implicated in osteoblast secretory functions.[15,16] However, the precise molecular mechanisms of 1,25D induction of regulated exocytosis in osteoblasts, as well as the product of 1,25D-sensitive secretion, remained at a speculative stage. We showed previously that rapid modulation of plasma membrane calcium and chloride channel activities by physiological concentrations of 1,25D couples to a significant increase of cell membrane electrical capacitance associated with exocytosis in primary osteoblasts expressing a functional VDR.[10] Osteoblasts, as well as a number of osteoblastic cell lines, express the SNARE (soluble N-ethylmaleimide-sensitive factor [NSF] attachment protein [SNAP] receptor) proteins molecular machinery required for regulated exocytosis.[17] Secretory granules and vesicles couple to the SNARE complex at the osteoblast plasma membrane and respond to mechanical and chemical stimuli by releasing a variety of products, including glutamate, prostaglandins, and ATP.[16–18] This suggests the existence of subpopulations of SNARE protein-coupled secretory structures in osteoblasts with the capacity to respond specifically to diverse stimuli.

Some of the products secreted by osteoblasts act locally in an autocrine/paracrine fashion.[16] It has been accepted for some time that exocytotic release of ATP, for example, occurs in response to mechanical stimulation in

The authors state that they have no conflicts of interest.

Department of Biochemistry, University of California, Riverside, California, USA.

osteoblasts.[16,18] On one hand, secreted ATP acts as a local signaling molecule through purinergic receptors P2X and P2Y expressed in the osteoblast plasma membrane.[19] On the other hand, rapid hydrolysis of extracellular ATP constitutes a source of inorganic phosphates, which have been implicated in the mineralization of the matrix.[16,20] In addition, extracellular ATP has been proposed to play a dual role in both stimulation and inhibition of osteoclast proliferation and activity depending on the local concentration of hormone at the single-cell surface level.[21] This results from the balance between local availability of the nucleotide—as a result of osteoblast exocytotic activities—and rapid degradation of ATP by extracellular nucleotidases.[22,23] In healthy bone tissue, low micromolar concentrations of extracellular ATP have been measured in relation with osteoclast maturation and bone resorption,[24] whereas higher micromolar concentrations have been correlated with reduction of osteoclast activity and the associated in vitro formation of resorption pits.[20] High ATP concentrations can be achieved in the immediate vicinity of actively secreting osteoblasts.

Whereas ATP secretion has been characterized in fair detail in relation with mechanotransduction of osteoblasts,[16,18] little is known on the molecular mechanisms of hormonal regulation of ATP exocytosis in bone-forming cells under static conditions. Here, we studied the hypothesis that, in the absence of mechanical stimulation, 1,25D induces a calcium-dependent regulated exocytosis of ATP through activation of an extranuclear VDR in osteoblasts. Rapid increase of extracellular ATP concentrations at the vicinity of the osteoblast surface promoted by 1,25D may contribute to bone formation and mineralization of the matrix. This may help explain, at least in part, bone anabolic functions of the steroid observed in vitro under static conditions.

MATERIALS AND METHODS

Chemicals

All chemicals used were purchased from Sigma (St. Louis, MO, USA), unless indicated otherwise. Calcium channel modulators nifedipine (2 μM) and S(−)Bay K8644 (0.5 μM), chloride channel blocker 5-nitro-2-(phenylpropylamino)-benzoate (NPPB, 300 μM), and calcium ionophores ionomycin (2 μM) and thapsigargin (3 μM) were used at the indicated final concentrations from stock solutions made in ethanol. Inhibitors of regulated exocytosis N-ethylmaleimide (NEM, 1 mM) and monensin (100 μM) were also prepared from stock solutions in ethanol. Chloride channel blocker 4,4′-diisothiocyanatostilbene-2,2′-disulfonic acid (DIDS, 200 μM final concentration) and fluorescent dye quinacrine (final concentration, 3 μM) stock solutions were made in water. Natural vitamin D_3 metabolites $1\alpha,25(OH)_2$vitamin D_3 (1,25D) and $25(OH)_2$ vitamin D_3 (25D) (Biomol Research laboratories, Plymouth, PA, USA), the synthetic analog $1\beta,25(OH)_2$vitamin D_3 (1β,25D, a generous gift from Dr. A. W. Norman, University of California, Riverside), and 17β-estradiol were stored as stock solutions in ethanol at −20°C in the dark.

Cell culture

Osteoblastic rat ROS 17/2.8 (kindly provided by Dr. A. W. Norman, University of California-Riverside) and human SAOS-2 cells (ATTC, Manasas, VA, USA), and primary mouse calvarial osteoblasts were cultured in Ham F-12 nutrient mixture containing 1 mM Glutamax (Invitrogen, Carlsbad, CA, USA), 5% FBS (Fisher, Pittsburgh, PA, USA), 5% Serum Plus (JRH Biosciences, Woodland, CA, USA), penicillin (100 U/ml), streptomycin (100 μg/ml), and 1.1 mM $CaCl_2$, at 37°C in a humidified 5% CO_2 atmosphere, essentially as described before.[8,25] Mouse calvarial osteoblasts were obtained as described previously.[10] Typically, ROS 17/2.8 and SAOS-2 cells were used 4–5 days after passage, at ~90% of confluency. Primary osteoblasts were allowed to proliferate for 2 wk. The culture medium was replaced by serum free medium 24 and 12 h before treatments for ROS 17/2.8 cells and primary osteoblasts, and SAOS-2 cells, respectively, also as described before.[8,22]

Quinacrine staining of ATP-containing cytoplasmic vesicles and time-lapse video microscopy

For imaging of real-time exocytosis, ROS 17/2.8 osteoblasts were grown on glass-bottom culture chambers (MatTek, Ashland, MA, USA) for 4 days, transferred to serum-free medium for 24 h, and stained with the fluorescent dye quinacrine (3 μM) for 30 min at 37°C. Cells were rinsed twice with Hank's buffered salt solution (HBSS). Cell manipulation was performed very gently to minimize any unintentional mechanical stimulation. Quinacrine-stained live osteoblasts were viewed with an Olympus IX50 fluorescence microscope at high magnification, using a FITC filter. Exocytosis was induced by means of gentle addition of each reagent to the HBSS bath. Single vesicle exocytosis was recorded as the rapid loss of fluorescence from quinacrine-stained individual secretory vesicles, because the dye diffused into the extracellular buffer on fusion of vesicles with the plasma membrane. Time-lapse sequences were recorded with a Spot Pursuit digital camera (Diagnostic Instruments, Sterling Heights, MI, USA) at scanning rates of 2 images/s for periods of up to 60 s.

Image analysis

We quantified the extent of exocytosis as a function of fluorescence loss from individual secretory vesicles over time by using in-home developed software. This software measured the fluorescence intensity of quinacrine-loaded vesicles selected by the experimenter as arbitrary fluorescence units (AFU) per pixel. Selection of vesicles took place on the basis of an arbitrary intensity threshold (100 AFU) defined by the experimenter. Fluorescence intensity was recorded continuously during the addition of the stimulus at a sampling rate of 2 frames/s for a length of time of 52 s. Changes in AFU values (expressed as percent AFU decrease) calculated between the beginning and the end of each recording were then classified according to a percent range defined by the experimenter. Losses of fluorescence intensity >75%, between 75% and 25%, and

<25% were defined as complete, partial, and no exocytosis, respectively. Histograms of frequency for the distribution of percentages of AFU decrease per vesicle were constructed for the comparative analysis of exocytotic events recorded in the absence and presence of different agents. The overall exocytosis rate obtained with different treatments was calculated as the slope of the linear function fitted to the graph that depicted the average AFU value obtained for all vesicles in each recording per sec.

Measurement of ATP concentration

Osteoblasts were plated at a density of 5,000 cells/cm^2 in 6-well plates and cultured as described above. ROS 17/2.8 cells and primary osteoblasts were serum starved for 24 h, and SaOS-2 cells were serum starved for 12 h 4–5 days after passage, at 90% confluency. On the day of the experiment, a circular area of 1 mm in diameter was drawn on the bottom of the dish, from which cells were scraped off. The culture medium was replaced by 1 ml of fresh serum-free medium, and the preparation was allowed to equilibrate for 1 h. Five hundred microliters of serum free medium was replaced by an equal volume of medium containing the reagent tested and incubated for 2 min. Medium (850 μl) was collected by gently resting the tip of a pipette on the cell-free marked area of the dish to reduce any possible release of ATP caused by mechanical stimulation of the cells. The concentration of ATP present in the collected medium was measured using a luciferase/luciferin luminescence ATP assay kit (Invitrogen, Carlsbad, CA, USA) according to the manufacturer's protocol. The assay is based on the conversion of D-luciferin into oxyluciferin and light by the enzyme luciferase in the presence of ATP. The resulting luminescence signal is proportional to ATP concentration in the reaction medium. Luminescence units were transformed into nanomolar concentration units of ATP relative to the protein concentration of the samples by means of a calibration curve generated for each separate luciferase assay, using a serial dilution of an ATP standard. Luminescence values were measured in a multidetection plate reader (Bio-Teck Instruments, Winoosky, VT, USA). Protein concentration of cell samples was measured with a protein assay kit from Bio-Rad (Hercules, CA, USA).

VDR knockdown

SiRNA knockdown of the VDR in ROS 17/2.8 and SAOS-2 osteoblasts was done essentially as described before.[25] Briefly, cells were grown in 6-well plates for 24 h and transfected at 80% confluency with 4 μg of a GenEclipse VDR siRNA construct or control vector siRNA in 500 μl Ham F-12 serum-free medium containing 5 μl Lipofectamine 2000 (Invitrogen), according to the manufacturer's protocol. Transfection medium was replaced by fresh serum-containing medium after 5 h. Cells were grown for 48 h in regular Ham F-12 medium and transferred to serum-free medium 12 h before use. VDR silencing was verified by Western blot analysis for VDR protein levels in siRNA VDR transfected and control vector-transfected cells.

Western blot analysis of VDR expression

Cell lysates were obtained in lysis buffer containing 50 mM Tris-HCl (pH 7.4), 150 mM NaCl, 2 mM EDTA, 25 mM NaF, 0.25% (wt./vol.) sodium deoxycholate, 1% (vol./vol.) NP-40, 0.2 mM Na_3VO_4, 1 mM 4-(2-aminoethyl)benzenesulfonyl fluoride hydrochloride (Pefabloc), 2 μg/ml leupeptin, and 2 μg/ml aprotinin as described elsewhere.[25] Cell lysates containing 20 μg of protein were loaded and separated on 10% (wt./vol.) SDS-PAGE gels and transferred to PVDF membranes. After blockade with 5% nonfat milk in Tris-buffered saline plus 0.1% (vol./vol.) Tween 20 (TBST), membranes were incubated with a primary antibody against VDR (Santa Cruz Biotechnology, Santa Cruz, CA, USA) raised in rabbit, at a 1:1000 dilution. Blots were probed with an antibody against α-vinculin (Santa Cruz Biotechnology) as a reference for protein loading between samples. The VDR primary antibody was detected with an Alexa Fluor 680 anti-rabbit secondary antibody (Invitrogen, Molecular Probes), and fluorescence was measured using an Odyssey scanner (LI-COR Biosciences, Lincoln, NE, USA). Blot density was digitalized and analyzed with the UnScan-It gel software (Silk Scientific, Orem, UT, USA).

Immunofluorescence and cell imaging

SAOS-2 cells grown on glass coverslips for 4 days were fixed with 3.7% formaldehyde for 20 min, permeabilized with ice-cold 95% ethanol for 5 min, and incubated in 5% goat serum in PBS (pH 7.4) for 1 h to block any nonspecific binding of the antibodies. Cells were incubated overnight at 4°C with a primary rabbit monoclonal anti- VDR antibody (C-20; Santa Cruz Biotechnology; 1:500 dilution in 5% goat serum in PBS), and a primary mouse polyclonal anti- chloride channel ClC-3 (Alomone Laboratories, Jerusalem, Israel; 1:300 dilution in PBS). Primary antibodies were visualized with Alexa 488–conjugated goat anti-rabbit and Cy3 goat anti-mouse secondary antibodies (Invitrogen; 1:500 dilution in PBS) for 2 h at room temperature. Subcellular co-localization of VDR and ClC-3 was studied with an Olympus IX50 inverted microscope. Images were captured with a Spot digital camera (Diagnostic Instruments, Sterling Heights, MI, USA) and analyzed with Simple PCI C-Imaging Systems software (Compix, Cranberry Township, PA, USA).

Statistical analysis

Data were expressed as means ± SE. The two-tailed Student's *t*-test with two sample unequal variance was used for statistical analysis, with $*p < 0.05$ and $**p < 0.01$ as significantly and highly significantly different, respectively.

RESULTS

1,25D induces vesicular exocytosis in ROS 17/2.8 osteoblastic cells

We showed previously with electrophysiology that nanomolar concentrations of the steroid hormone 1,25D induce a rapid (within 1 min) capacitance response associated with

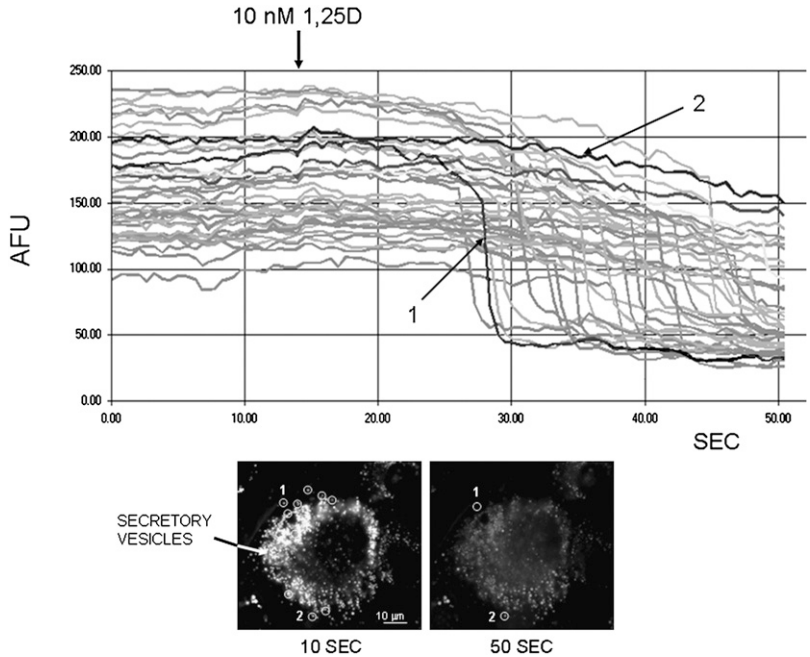

FIG. 1. 1,25D induces exocytotic release from quinacrine-loaded secretory vesicles in osteoblastic ROS 17/2.8 cells. Fluorescence intensity (expressed as arbitrary fluorescence units [AFUs]) recorded continuously from 45 individual secretory vesicles in a ROS 17/2.8 osteoblast during the addition of 10 nM 1,25D to the extracellular bath. Quinacrine-stained vesicles were selected from the image of an osteoblast shown in the bottom left panel. Continuous recording of fluorescence intensity was done over 52 s; 1,25D was added at the time indicated by the arrow, ~14 s after the beginning of the recording. Nine of the selected areas are indicated with circles drawn on the image on the left, which depicts the osteoblast immediately before treatment with the 10 nM 1,25D, at time 10 s from the beginning of the recording. The image on the right shows the same osteoblast after exocytotic release of quinacrine, at the end of the recording. The average AFU intensity of each selected area was measured every 500 ms. Highlighted for comparative purposes are traces obtained for a vesicle undergoing complete exocytosis (labeled 1, intensity decrease from ~100 to <50 AFU about 27 s into the recording), and a vesicle that did not undergo exocytosis (labeled 2, fluorescence intensity remained between 200 and 250 AFU during the entire length of the experiment).

exocytosis in primary calvarial osteoblasts[10] and osteosarcoma ROS 17/2.8 cells[11] expressing a functional VDR. Here, we used high-resolution video imaging to record for the first time 1,25D induction of individual exocytotic events in ROS 17/2.8 cells. ROS 17/2.8 cells, which retain a phenotype characteristic of fully differentiated osteoblasts, have been used extensively for the study of membrane-initiated nongenotropic actions of 1,25D.[8,12,25,26]

Figure 1 shows snapshots of a single live ROS 17/2.8 osteoblast stained with quinacrine, a fluorescent dye with affinity for the highly acidic microenvironment of secretory vesicles, immediately before (left image, 10 s) and after (right image, 50 s) treatment with 10 nM 1,25D. Exocytosis of quinacrine-loaded secretory vesicles has been studied before in relation with secretory responses of osteoblasts to mechanical stimulation.[16,19] To study the hypothesis that physiological concentrations of 1,25D promote exocytosis of 1,25D-sensitive secretory vesicles in the absence of mechanical stimulation in osteoblasts, we video recorded the exocytotic release of quinacrine from individual vesicles induced by an acute treatment with 1,25D. Single exocytotic events were detected as a localized, rapid loss of fluorescence intensity because of diffusion of quinacrine into the extracellular medium in the area corresponding to individual secretory vesicles. Figure 1 depicts the decrease of fluorescence intensity (expressed as AFU) measured over 52 s for 45 individual secretory vesicles selected from the picture shown in the bottom left panel. We found that a large subpopulation of quinacrine-loaded organelles responded to treatment with 10 nM 1,25D by rapidly releasing their fluorescent content. We measured a significant, abrupt 50–80% reduction of fluorescence intensity in ~80% of stained vesicles 20–30 s after the addition of 10 nM 1,25D to the extracellular medium.

Figure 2 shows the quantitative analysis of 1,25D stimulation of quinacrine release from a pool of secretory vesicles in ROS 17/2.8 cells. We constructed histograms of frequency for the distribution of the average percent decrease of fluorescence intensity (average AFU decrease) or percent extent of exocytosis for 100 selected vesicles in cells subjected to different treatments. For the construction of the histograms, fluorescent areas corresponding to different secretory vesicles were selected on the basis of the average AFU value measured for all pixels contained in each selected area, as described in the Materials and Methods section. We selected vesicles with an average AFU equal to or higher than an arbitrary threshold AFU value of 100 set by the experimenter, as shown in the images on the left. Figure 2A shows histograms for the distribution of the percent extent of exocytosis obtained after treatment with 1 and 10 nM 1,25D, nonstimulatory controls with HBSS (control for basal, unintentional mechanical

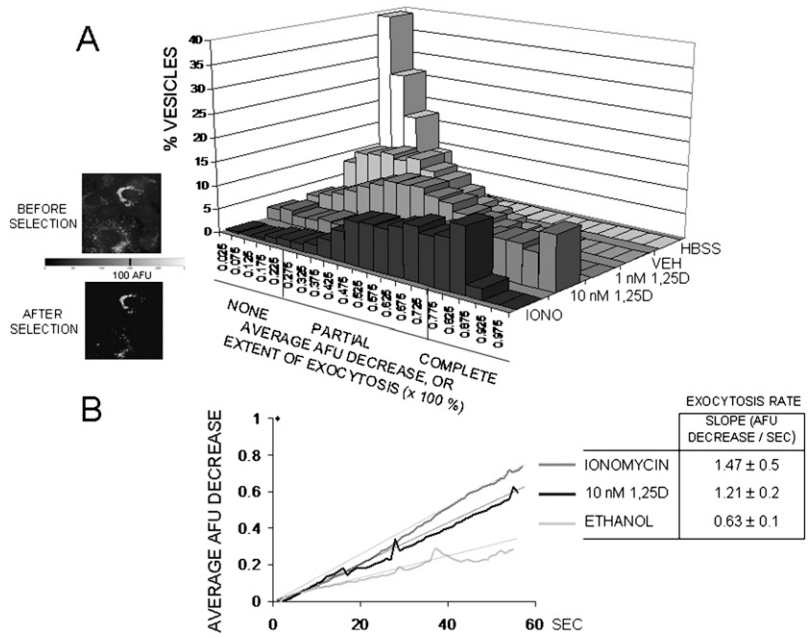

FIG. 2. Quantitative analysis of exocytotic events in ROS 17/2.8 osteoblasts. (A) Histograms for the distribution of the percent decrease of fluorescence intensity (AFU)—also expressed as extent of exocytosis (× 100%)—measured from 100 vesicles selected from images similar to the one shown in Fig. 1. Treatments included control for the addition of HBSS buffer, 0.01% ethanol (vehicle), 1 nM and 10 nM 1,25D, and 2 μM ionomycin. The extent of exocytosis was arbitrarily classified into three categories according to the magnitude of the reduction of fluorescence intensity of the selected vesicles. These categories comprised no exocytosis (for vesicles with AFU decrease <25%), partial exocytosis (AFU decrease between 25% and 75%), and complete exocytosis (AFU decrease >75%). (Left) Fluorescent images of osteoblasts before (top) and after (bottom) application of an arbitrary intensity threshold of 100 AFU. Only fluorescence areas with intensity values ≥100 AFU were used in the construction of the histograms. (B) Average fluorescence intensity (AFU) decrease of all analyzed selected areas during the length of the experiment (52 s) obtained for 0.01% ethanol (for vehicle control), 10 nM 1,25D, and 2 μM ionomycin treatments. (Table) Values obtained for the exocytosis rate with different treatments, calculated from the slope of the linear regression fitted to continuous data, and expressed as AFU decrease per second.

stimulation caused by manipulation) and ethanol 0.01% (control for vehicle), and a positive stimulatory control with the calcium ionophore ionomycin (2 μM), on different ROS 17/2.8 cell cultures. Histograms shown in Fig 2 are representative of three to five separate experiments conducted for each treatment. We found that the addition of 10 nM 1,25D to the bath induced the majority of secretory vesicles to lose 75% or more of their fluorescence compared with the effects promoted by a lower concentration of hormone (1 nM) and controls for vehicle and medium and was comparable with the extent of exocytosis caused by treatment with ionomycin.

Next, with the intention to facilitate comparison among treatments, we subdivided the range of values measured for the percent average AFU decrease of vesicles (0–100%), or percent extent of exocytosis, into three categories. A loss of fluorescence intensity of at least 75% was defined as representative of vesicles undergoing complete exocytosis, between 25% and 75% average AFU decrease as vesicles undergoing partial exocytosis, and <25% average AFU decrease as vesicles undergoing no exocytosis. Table 1 shows the values obtained for the percentage of vesicles that fell into each category for the different treatments shown in the histograms in Fig. 2. Treatment of ROS 17/2.8 cells with 10 nM 1,25D caused a majority of vesicles to undergo either complete (41.1%) or partial (46.2%) exocytosis with an overall average fluorescence reduction of 86 ± 7% (n = 100 vesicles). Similarly, 2 μM ionomycin caused an average fluorescence decrease of 72 ± 5%, as measured for all sampled vesicles (n = 100), with most (70.8%) vesicles undergoing partial exocytosis. On the other hand, 1 nM 1,25D caused an average loss of fluorescence intensity of only 40 ± 5% (n = 100), with most responsive vesicles (74.5%) carrying out partial exocytosis only. The

TABLE 1. Extent of Exocytosis Induced by 1,25D Treatment in ROS 17/2.8 Cell Cultures

	No exocytosis	*Partial exocytosis*	*Complete exocytosis*	*Overall average AFU decrease (%)*
AFU decrease	0–25%	25–75%	>75%	
Medium	96.4 ± 0.5	3.6 ± 0.5	0	8 ± 2
Vehicle	62.6 ± 0.3	37.3 ± 0.4	0.1 ± 0.3	22 ± 3
1 nM 1,25D	24.7 ± 0.2	74.5 ± 0.4	0.7 ± 0.4	40 ± 5
10 nM 1,25D	12.7 ± 0.5	46.2 ± 0.3	41.1 ± 0.2	86 ± 7
Ionomycin	3.5 ± 0.6	70.8 ± 0.2	25.7 ± 0.2	72 ± 5

Percent of vesicles undergoing no, partial, or complete exocytosis measured in n = 4 representative experiments for the indicated treatments, as explained in Fig. 2. Vehicle: ethanol 0.01%, ionomycin 2 μM. The overall average AFU decrease was calculated from n = 100 vesicles. All values in the table are percentages.

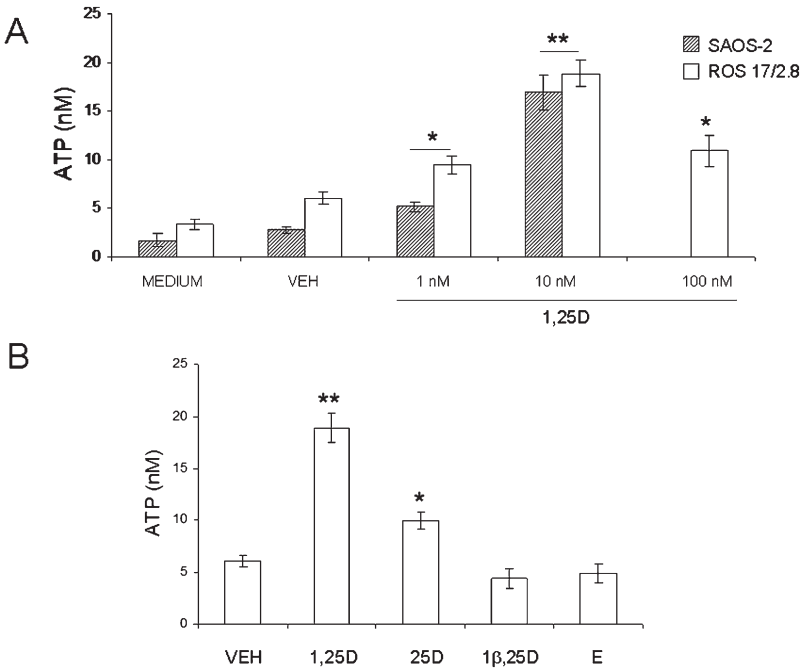

FIG. 3. 1,25D stimulates ATP release in a dose-dependent manner and is selective for the hormone in static osteoblasts. (A) Values of ATP concentration (expressed in nM) measured in the extracellular bath 2 min after the addition of 1–100 nM 1,25D to SAOS-2 and ROS 17/2.8 cultures compared with controls obtained for the addition of medium and 0.01% ethanol (VEH). (B) Values of ATP concentration (expressed in nM) measured in the extracellular bath of ROS 17/2.8 cultures 2 min after treatment with the natural metabolite 25D (10 nM), the synthetic antagonist 1β,25D (10 nM) in combination with 10 nM 1,25D, and 10 nM 17β-estradiol (E) compared with ATP values obtained for a control for vehicle (0.01% ethanol). Medium was collected 2 min after the indicated treatments, and ATP concentration was measured in the bulk extracellular solution using an ATP-sensitive luciferin-luciferase reaction and normalized to the protein concentration of the samples. Data shown are mean values ± SE obtained from n = 6–48 independent experiments. *$p < 0.05$; **$p < 0.01$.

addition of ethanol and medium caused an average fluorescence intensity decrease of only 22 ± 3% and 8 ± 2%, respectively (n = 100), and comprised vesicles that mostly did not undergo any exocytosis (62.6% and 96.4%, respectively).

Next, we calculated the rate at which the average AFU for all sampled vesicles decreased over 52 s of recording or speed at which maximal exocytosis was achieved in response to different treatments. Figure 2B depicts the average AFU decrease value measured over time when ROS 17/2.8 cells were treated with 10 nM 1,25D, compared with 2 μM ionomycin, which quickly depletes calcium from internal cellular stores, and control for vehicle. The average exocytosis rate corresponding to each treatment was calculated from the slope of a linear function fitted to the raw curves. We found that 10 nM 1,25D induced exocytosis at a rate of 1.21 ± 0.2 average AFU lost per second in n = 4 representative experiments, which was significantly higher than 0.63 ± 0.1 AFU per second induced by ethanol, but similar to 1.47 ± 0.5 AFU per second triggered by 2 μM ionomycin, suggesting that availability of Ca^{2+} in the cell cytoplasm plays a role in 1,25D induction of exocytosis in osteoblasts.

ATP is secreted in response to 1,25D treatment in static osteoblasts

Exocytotic release of ATP has been shown previously to be induced by mechanical stimulation of osteoblasts.[16] To study the hypothesis that nanomolar concentrations of 1,25D specifically stimulate rapid exocytosis of ATP in the absence of mechanical stimulation in osteoblasts, we measured extracellular ATP concentrations under static conditions after acute treatment with hormone. As described in the Materials and Methods section, we used a luciferin/luciferase-based bioluminescence assay that directly reflects ATP concentration in the medium. ATP concentration values were normalized to total protein concentration in the cell cultures, which averaged 1000 ± 100 μg/ml. Figure 3A shows extracellular ATP levels detected in ROS 17/2.8 and SAOS-2 cultures 2 min after the addition of increasing concentrations (1–100 nM) of 1,25D. We measured a basal release of ATP of 1.75 ± 0.67 (n = 6) and 3.38 ± 0.53 nM (n = 11) in SAOS-2 and ROS 17/2.8 cells, respectively, 2 min after the addition of 500 μl of fresh medium as control for any possible unintentional mechanical stimulation caused by manipulation of the cultures during the experiment. Similarly, the addition of an equal volume of ethanol 0.01% as vehicle control did not cause any significant change in basal ATP concentrations (2.75 ± 0.39 nM, n = 14, and 6.09 ± 0.58 nM, n = 22, in SAOS-2 and ROS 17/2.8 cells, respectively). As seen in Fig. 3, 1–100 nM 1,25D evoked a dose-dependent stimulation of ATP secretion in osteoblasts, with a maximal response of ~6.2 ± 0.3-fold and 3.1 ± 0.2-fold for SAOS-2 and ROS 17/2.8 cells, respectively, obtained with 10 nM of hormone (16.93 ± 1.82 nM, n = 11; $p < 0.01$ for SAOS-2 cells; 18.89 ± 1.39 nM, n = 48, $p < 0.01$ for ROS 17/2.8 cells) in respect to vehicle. Biphasic effects of 1,25D have been reported previously in relation with nongenotropic effects of the steroid, including activation of calcium and chloride channel activities in ROS 17/2.8 cells.[10] Next, we measured the stimulation of ATP secretion by 10 nM 1,25D in primary osteoblasts isolated from mouse calvaria. We found a significant 4.2 ± 0.3-fold increase of extracellular ATP concentration (12.73 ± 0.52 nM) induced by 1,25D compared with vehicle (3.06 ± 0.41 nM ATP) within 2 min. Results obtained for the three osteoblast systems studied are summarized in Table 2.

To evaluate the specificity of 1,25D induction of ATP release in osteoblasts, we measured extracellular ATP

TABLE 2. ATP Concentration Values Obtained With 10 nM 1,25D Compared With Vehicle in Three Osteoblastic Cell Systems Studied

	Basal	*1,25D*	*Fold increase*
SAOS-2	2.75 ± 0.39	16.93 ± 1.83*	6.2 ± 0.3
Si RNA VDR SAOS-2	2.42 ± 0.390.23	2.81 ± 0.33	1.2 ± 0.1
ROS 17/2.8	6.09 ± 0.58	18.89 ± 1.39*	3.1 ± 0.2
Si RNA ROS 17/2.8	5.71 ± 0.39 0.36	7.08 ± 0.39 0.41	1.2 ± 0.1
Primary osteoblasts	3.06 ± 0.41	12.73 ± 0.52*	4.2 ± 0.3
VDR KO primary osteoblasts	3.43 ± 0.24	4.25 ± 0.43	1.2 ± 0.2

ATP concentration is expressed in nM and has been normalized to total protein concentration in the cell samples. Basal corresponds to vehicle control (ethanol 0.01%), and 12,5D concentration is 10 nM. Data are mean values ± SE of n = 18–48 experiments.

* $p < 0.01$.

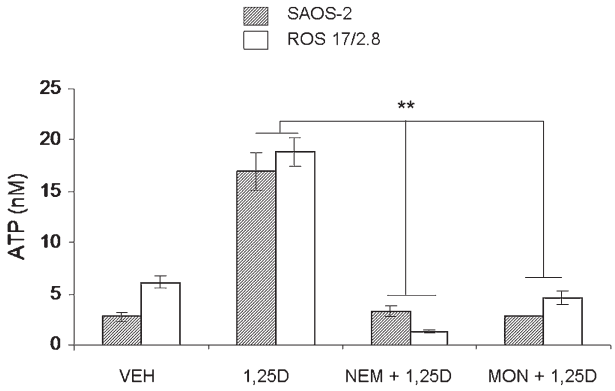

FIG. 4. 1,25D-induced ATP release is vesicular. Values of ATP concentration (expressed in nM) measured in the extracellular bath 2 min after the addition of 10 nM 1,25D alone or in the presence of 1 mM NEM or 100 μM monensin (1 h before treatment) to SAOS-2 and ROS 17/2.8 cell cultures. Data shown are mean values ± SE obtained from n = 6–24 independent experiments. *$p < 0.05$; **$p < 0.01$.

concentration after treating ROS 17/2.8 cells with the natural metabolite $25(OH)_2$vitamin D_3 (25D), the synthetic antagonist for nongenotropic responses $1\beta,25(OH)_2$vitamin D_3 (1β,25D),[27] and the steroid hormone 17-β estradiol (E), at a final concentration of 10 nM each, and compared them with ATP levels obtained after treatment with 10 nM 1,25D. As shown in Fig. 3B, we measured no significant stimulation of ATP secretion by 10 nM 1,25D when ROS 17/2.8 cells were pretreated with the stereoisomer 1β,25D (4.42 ± 0.86 nM, n = 14) with respect to vehicle control. On the other hand, 10 nM 25D caused a significant 3.6 ± 0.2-fold elevation of extracellular ATP (9.95 ± 0.78 nM, n = 13, $p < 0.05$), although considerably lower than the elevation of ATP concentration obtained with 10 nM 1,25D. On the other hand, the steroid hormone 17-β estradiol did not induce any significant stimulation of ATP release in ROS 17/2.8 osteoblasts (4.91 ± 0.89 nM, n = 13). Taken together, these results showed specificity of the ATP secretory response to 1,25D over other steroid hormones, as well as higher responsiveness to the natural most active form of the secosteroid compared with other natural forms of the hormone, suggesting the involvement of a classic VDR.

Mechanical stimulation of ATP release in osteoblasts is vesicular and involves a SNARE complex.[16,19] To study whether 1,25D-mediated exocytosis of ATP also originates from the docking and fusion of ATP-containing secretory vesicles to the osteoblast plasma membrane through a SNARE protein complex expressed in osteoblasts,[17] we used pharmacological agents known to interfere with vesicular formation and fusion. As shown in Fig. 4, a 1-h pretreatment of ROS 17/2.8 and SAOS-2 cells with 1 mM NEM, which prevents fusion of secretory vesicles to the plasma membrane, or with 100 μM monensin, which interferes with vesicle formation from the Golgi apparatus,[28] caused complete inhibition of 1,25D induction of ATP release, thus verifying that 1,25D-stimulated ATP release is vesicular.

A classic VDR is required for 1,25D induction of exocytotic release of ATP

We reported previously that an extranuclear VDR is required for 1,25D stimulation of electric currents associated with exocytotic activities in osteoblasts.[10] To study whether a VDR is involved in nongenotropic 1,25D induction of ATP exocytosis in osteoblasts, we measured extracellular ATP concentration after 1,25D treatment of ROS 17/2.8 and SAOS-2 cells in which the native VDR was silenced with siRNA technology.[25,29] To verify VDR silencing, lower expression of the VDR protein detected with Western blot analyses was found in native ROS 17/2.8 and SAOS-2 cells compared with VDR knockdown cells. As shown in Figs. 5A and 5B, we measured a significant inhibition of 1,25D induction of ATP release in VDR-silenced ROS 17/2.8 and SAOS-2 cells (labeled –VDR in the figure) compared with control siRNA vector transfected cells. Similarly, primary calvarial osteoblasts obtained from a VDR knockout mouse[10] did not respond to stimulation with 10 nM 1,25D, as summarized in Table 2. Taken together, these results show that a classic VDR is required for rapid, nongenotropic 1,25D-induction of exocytotic ATP release in osteoblasts and agree with electrophysiological results reported previously by our group in primary osteoblasts.[10]

1,25D induction of ATP release in static osteoblasts is calcium dependent

Vesicular exocytosis has been shown to be a Ca^{2+}-dependent process in a variety of cell systems.[30,31] Clusters of Ca^{2+}-permeable ion channels including L-Ca channels are found in the vicinity of exocytotic vesicles docked to the plasma membrane of secretory cells. In addition, Ca^{2+} released from intracellular stores contributes to the mobilization of secretory vesicles and onset of exocytosis.[32] Osteoblasts express voltage-gated L-Ca channels at the plasma membrane that respond to 1,25D modulation.[33,34] In the

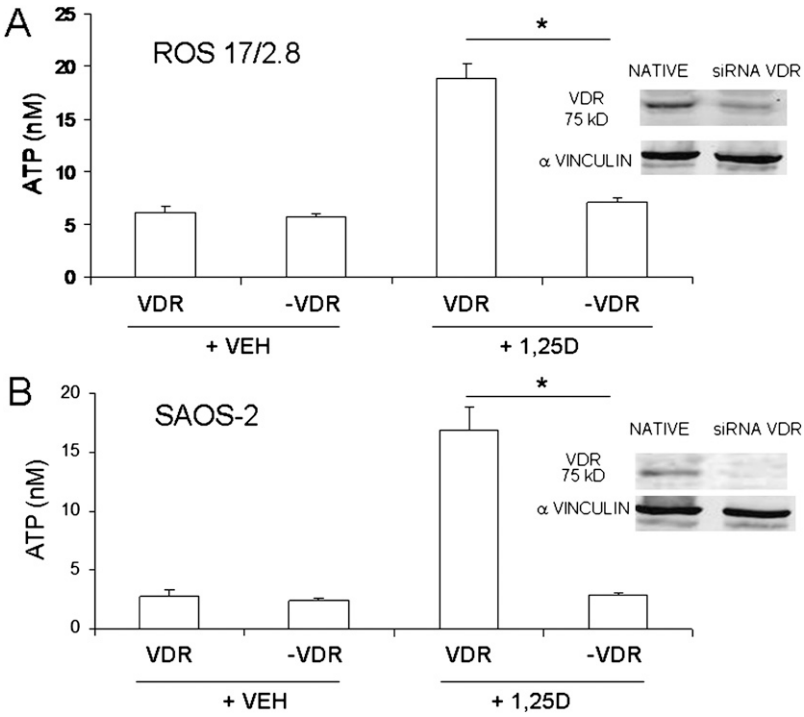

FIG. 5. 1,25D induction of exocytotic ATP release requires a classic VDR in osteoblasts. ATP concentration values (expressed in nM) measured in the extracellular bath 2 min after the addition of 10 nM 1,25D or 0.01% ethanol (vehicle control) to ROS 17/2.8 (A) and SAOS-2 (B) cell cultures expressing the native VDR vs. cultures in which the VDR was silenced (−VDR). (Right panels, top and bottom) Western blot analysis for VDR expression in native (control vector-transfected) and siRNA VDR-silenced osteoblasts; α-vinculin was used as a loading control. Data shown are mean values ± SE obtained from n = 5–6 independent experiments. *$p < 0.05$.

presence of the hormone, L-Ca channels exhibit longer open states,[12] thus allowing higher Ca^{2+} influxes and subsequent elevation of cytoplasmic Ca^{2+} in the immediate surroundings of the channel. In addition, hormone 1,25D elevates intracellular Ca^{2+} by depleting internal stores through nongenotropic mechanisms that involve activation of phospholipase C in osteoblasts.[6,7,12,13,35] We showed previously that 1,25D-stimulated whole cell capacitance changes, which are a measure of exocytosis, depend on the availability of intracellular calcium.[36] To evaluate whether 1,25D stimulation of ATP release in static, nonmechanically stimulated osteoblasts occurs in response to 1,25D-promoted elevation of intracellular calcium through opening of plasma membrane L-Ca channels and/or depletion from internal stores, we measured extracellular ATP concentration after treatment of ROS 17/2.8 cells with L-Ca channel modulators and stimulators of calcium release from the endoplasmic reticulum.

Figure 6A shows that a 2-min treatment with the specific L-Ca channel agonist 0.5 μM S(−)Bay K8644 induced a significant 2.8-fold increase of secreted ATP (17.32 ± 2.49 nM, n = 15, $p < 0.01$) with respect to vehicle control (6.09 ± 0.58 nM, n = 22), thus mimicking the effect of 10 nM 1,25D (19.32 ± 1.43 nM, n = 49, $p < 0.01$). On the other hand, preincubation of ROS 17/2.8 cells with the L-Ca channel antagonist nifedipine (2 μM) completely abolished 1,25D induction of ATP exocytosis, indicating that L-Ca channel activation is required for 1,25D stimulation of ATP exocytosis. In addition, the calcium ionophores ionomycin (2 μM) and thapsigargin (3 μM), which act at the endoplasmic reticulum, significantly stimulated ATP secretion (3.7- and 4.6-fold, respectively) with respect to vehicle, in an extent similar to 1,25D stimulation, indicating that exocytotic release of ATP responds to multiple sources of cytoplasmic Ca^{2+} in osteoblasts. Taken together, our results suggest that 1,25D potentiation of calcium signals seems to be a required step in the sequence of rapid molecular events taking place at the plasma membrane level and its proximity that lead to 1,25D stimulation of ATP exocytosis in static osteoblasts.

1,25D stimulation of ATP secretion involves chloride channel activation in osteoblasts

Voltage-gated chloride channels are involved in regulated exocytosis in a variety of secretory cells.[37,38] Chloride ions provide the electric shunt necessary for H^+ to be pumped into secretory vesicles. We showed previously that nanomolar concentrations of 1,25D potentiate outwardly rectifying chloride currents in ROS 17/2.8 cells within the first 2 min,[8,39] which couple to exocytosis[40] in osteoblasts expressing a functional VDR.[10] Here, we studied the hypothesis that 1,25D potentiation of chloride channel activities is required for 1,25D induction of ATP exocytosis in osteoblasts. Figure 6B shows extracellular ATP concentrations measured 2 min after the addition of 10 nM 1,25D in the absence and presence of 300 μM NPPB and 200 μM DIDS, two specific blockers of voltage-gated chloride channels, in ROS 17/2.8 and SAOS-2 osteoblasts. We found that pre-incubation with the blockers abolished 1,25D regulated ATP secretion, indicating that voltage-gated chloride channels are involved in 1,25D-sensitive exocytotic functions in osteoblasts. In addition, we found that voltage-gated chloride channels and VDR co-localize in the vicinities of the plasma membrane and secretory vesicles in SAOS-2 osteoblasts, as shown in Fig. 6C.

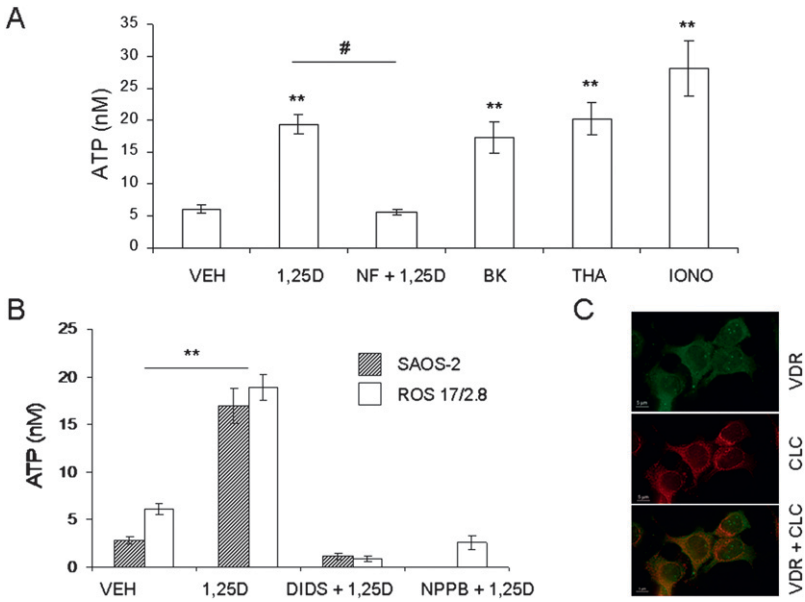

FIG. 6. 1,25D induction of ATP secretion is calcium dependent and requires chloride channel activation. (A) ATP concentration values (expressed in nM) measured in the extracellular bath 2 min after the addition of 0.01% ethanol (VEH), 10 nM 1,25D alone or in the presence of the L-Ca channel blocker nifedipine (NF, 2 μM), L-Ca channel agonist S(−) Bay K8644 (BK, 0.5 μM), and calcium ionophores thapsigargin (THA, 3 μM) and ionomycin (IONO, 2 μM) to ROS 17/2.8 cells. (B) ATP concentration values (expressed in nM) measured in the extracellular bath 2 min after the addition of 0.01% ethanol (VEH), 10 nM 1,25D alone or in the presence of chloride channel blockers 200 μM DIDS, or 300 μM NPPB to SAOS-2 and ROS 17/2.8 cell cultures. Data shown are mean values ± SE obtained from $n = 11$–22 independent experiments. $^{**}p < 0.01$; $^{\#}p < 0.005$. (C) Immunocytochemistry images obtained for VDR (green) and chloride channel (red) subcellular localization in SAOS-2 osteoblasts. Yellow denotes co-localization.

DISCUSSION

The physiological significance of nongenotropic effects of the steroid hormone 1,25D in relation with bone formation remains only partially understood. Whereas rapid (seconds to minutes) 1,25D actions on osteoblast ion channels, protein kinases, and calcium signals have been described with fair detail during the course of the last decade,[5,7,9] there is no generalized consensus on the precise physiological implications at the tissue and organism level. Most accepted at present is the idea that cytoplasmic cascades triggered by nongenotropic actions of 1,25D bound to an extranuclear VDR cross-talk to the nucleus to modulate the expression of genes involved in osteoblast proliferation, survival, and apoptosis.[13,25,29,41] Under this framework, 1,25D rapid extra nuclear actions translate ultimately into bone tissue formation within a time frame of hours to days, at least as measured with cell culture systems.

We documented previously that nongenotropic effects of 1,25D taking place at the osteoblast plasma membrane and its proximity require a VDR and affect the cell's ionic and electrical state.[11] In this study, we showed that membrane-initiated electrical actions of the steroid lead to an immediate physiological response at the cell level consisting of a regulated exocytosis of ATP, which may be involved in the deposition of new bone materials. We described here for the first time rapid 1,25D induction of ATP secretion in osteoblasts and showed that the physiological significance of 1,25D stimulation of cytosolic Ca^{2+} and Cl^- channel activities resides, at least in part, in the regulation of exocytosis. Although exocytotic ATP release has been shown before to occur in response to mechanical stimulation in osteoblasts,[12] steroid hormone induction in the absence of a mechanical stimulus is a novel concept, which may have potential biomedical implications.

Here, we used time-lapse video microscopy and measured extracellular ATP concentrations to study dose dependence, specificity, VDR involvement, and calcium and chloride requirement in 1,25D regulation of exocytosis. We found that at least 80% of quinacrine-stained vesicles underwent exocytosis with 1,25D treatment (Figs. 1 and 2). The remaining pool of stained vesicles, which did not respond to 1,25D treatment, are probably nonsecretory organelles with an affinity for the dye or nonmatured vesicles not ready for exocytosis, and therefore they do not constitute a readily releasable pool.

We observed that, whereas treatment of cells with ionomycin—which quickly depletes internal calcium stores—caused the fastest exocytotic response (see table inserted in Fig. 2B), it induced complete exocytosis in only 25.7% of the stained vesicles compared with 41.1% induced by 10 nM 1,25D (Table 1). This indicated that a mechanism different from, or in addition to, an internal source of calcium might be involved in 1,25D stimulation of exocytosis. In support of this, we found that blockade of L-Ca channels with nifedipine completely abolished 1,25D induction of ATP secretion in ROS 17/2.8 cells (Fig. 6A), which showed that opening of voltage-gated calcium channels is a required step in 1,25D regulation of exocytosis.

Previous work by our group on primary osteoblasts isolated from a VDR knockout (KO) mouse showed that a classic VDR is required for 1,25D stimulation of electric currents coupling to exocytosis in the bone-forming cells.[10] In agreement with these previous observations, we showed here that 1,25D failed to stimulate any significant secretion of ATP in static calvarial osteoblasts isolated from the VDR KO mouse and that silencing of the native VDR expressed in a rat and a human osteoblastic cell line abolished 1,25D induction of ATP secretion under static conditions, verifying the involvement of an extranuclear VDR in membrane-initiated actions of 1,25D. Although the precise series of molecular events has not been completely elucidated yet, we propose from our results that 1,25D interacts with a cytoplasmic VDR, which, on one

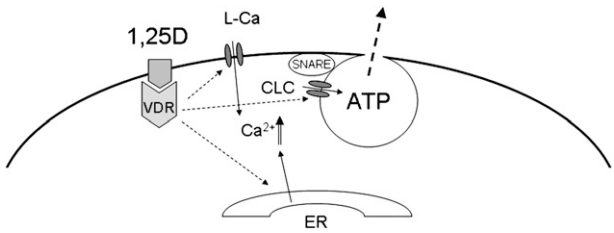

FIG. 7. Model proposed for 1,25D nongenotropic induction of ATP exocytosis in static osteoblasts. 1,25D interacts with an extranuclear VDR located at the cytoplasm in close proximity with the plasma membrane. Activated VDR induces L-Ca and chloride (ClC) channel opening, as well as release of calcium from internal stores (ER, endoplasmic reticulum). Ca^{2+} elevation in the most external layers of the cytoplasm activates a SNARE complex linked to a 1,25D-sensitive readily releasable pool of secretory vesicles containing ATP, which is secreted into the extracellular medium on rapid formation of a fusion pore.

hand, activates L-Ca and chloride channels present in the exocytotic complex through mechanisms that we described previously,[9] and on the other hand, induces calcium release from internal stores through rapid signaling described previously by others.[6,7,35] Our proposed model is shown in Fig. 7.

Extracellular ATP plays a relevant role in the bone microenvironment. ATP released by osteoblasts exerts an autocrine/paracrine signaling involved in the modulation of multiple functions related to the state of the bone matrix at remodeling sites.[16,20,22] Extracellular ATP is rapidly hydrolyzed by nucleotidases located in the extracellular matrix, yielding PPi. As a consequence, local concentrations of extracellular ATP vary rapidly. Different effects on the mineralization state of the bone matrix surrounding osteoblasts have been associated with changing ATP concentrations.[42] In our study, extracellular ATP concentrations ranging 5–30 nM have been measured from a 1 ml bulk solution on stimulation with 1,25D. It would be fair to infer that ATP concentrations in the immediate vicinity of the osteoblast surface (within a distance of few micrometers from exocytotic releasing sites) may be significantly higher, possibly ranging within micromolar values, at which bone mineralization is stimulated.[20]

In summary, we showed for the first time that, in the absence of mechanical stimulation, hormone 1,25D induces a regulated secretion of ATP in osteoblasts through interaction with an extranuclear VDR and potentiation of rapid calcium and chloride signals required for vesicle fusion and exocytotic release. Our findings may have important implications in bone biology and provide information for a better understanding of hormonal induction of osteogenesis under static conditions. They may also contribute to future identification of molecular targets for the treatment of bone pathologies characterized by decreased bone mass and reduced mineralization.

ACKNOWLEDGMENTS

The authors thank Elmer Hillo and Dr. Navin Twarkavi for technical support with imaging capture and processing and software development, respectively. This work was supported by NIH Grant DK071115 to L.P.Z.

REFERENCES

1. Aubin JE, Heersche JNM 1997 Vitamin D and Osteoblasts. Academic Press, San Diego, CA, USA.
2. Kraichely DM, MacDonald PN 1998 Transcriptional activation through the vitamin D receptor in osteoblasts. Front Biosci **3:**D821–D833.
3. Huhtakangas JA, Olivera CJ, Bishop JE, Zanello LP, Norman AW 2004 The vitamin D receptor is present in caveolae-enriched plasma membranes and binds 1α,25(OH)$_2$-vitamin D_3 in vivo and in vitro. Mol Endocrinol **18:**2660–2671.
4. Farach-Carson MC, Sergeev IN, Norman AW 1991 Nongenomic actions of 1α,25(OH)$_2$-vitamin D_3 in rat osteosarcoma cells: Structure-function studies using ligand analogs. Endocrinology **129:**1876–1884.
5. Boyan BD, Sylvia VL, Dean DD, Pedrozo H, Del Toro F, Nemere I, Posner GH, Schwartz Z 1999 1α,25(OH)$_2$-vitamin D_3 modulates growth plate chondrocytes via membrane receptor-mediated protein kinase C by a mechanism that involves changes in phospholipid metabolism and the action of arachidonic acid and PGE2. Steroids **64:**129–136.
6. Lieberherr M 1987 Effects of vitamin-D_3 metabolites on cytosolic free calcium in confluent mouse osteoblasts. J Biol Chem **262:**13168–13173.
7. Civitelli R, Kim YS, Gunsten SL, Fujimori A, Huskey M, Avioli LV, Hruska KA 1990 Nongenomic activation of the calcium message system by vitamin D metabolites in osteoblast-like cells. Endocrinology **127:**2253–2262.
8. Zanello LP, Norman AW 1997 Stimulation by 1α,25(OH)$_2$-vitamin D_3 of whole cell chloride currents in osteoblastic ROS 17/2.8 cells: A structure-function study. J Biol Chem **272:**22617–22622.
9. Zanello LP, Norman AW 2003 Multiple molecular mechanisms of 1α,25(OH)$_2$-vitamin D_3 rapid modulation of three ion channel activities in osteoblasts. Bone **33:**71–79.
10. Zanello LP, Norman AW 2004 Rapid modulation of osteoblast ion channel responses by 1α,25(OH)$_2$-vitamin D_3 requires the presence of a functional vitamin D nuclear receptor. Proc Natl Acad Sci USA **101:**1589–1594.
11. Zanello LP, Norman AW 2004 Electrical responses to 1α,25(OH)$_2$-vitamin D_3 and their physiological significance in osteoblasts. Steroids **69:**561–565.
12. Caffrey JM, Farach-Carson MC 1989 Vitamin D_3 metabolites modulate dihydropyridine-sensitive calcium currents in clonal rat osteosarcoma cells. J Biol Chem **264:**20265–20274.
13. Xiaoyu Z, Payal B, Melissa O, Zanello LP 2007 1α,25(OH)$_2$-vitamin D_3 membrane-initiated calcium signaling modulates exocytosis and cell survival. J Steroid Biochem Mol Biol **103:**457–461.
14. Jorgensen NR, Henriksen Z, Brot C, Eriksen EF, Sorensen OH, Civitelli R, Steinberg TH 2000 Human osteoblastic cells propagate intercellular calcium signals by two different mechanisms. J Bone Miner Res **15:**1024–1032.
15. Zanello LP, Norman AW 2004 Steroid hormone-regulated exocytosis in osteoblasts. Steroids **86:**171–175.
16. Genetos DC, Geist DJ, Liu D, Donahue HJ, Duncan RL 2005 Fluid shear-induced ATP secretion mediates prostaglandin release in MC3T3-E1 osteoblasts. Bone **20:**41–49.
17. Bhangu PS, Genever PG, Spencer GJ, Grewal TS, Skerry TM 2001 Evidence for targeted vesicular glutamate exocytosis in osteoblasts. Bone **29:**16–23.
18. Romanello M, Pani B, Bicego M, D'Andrea P 2001 Mechanically induced ATP release from human osteoblastic cells. Biochem Biophys Res Commun **289:**1275–1281.
19. Romanello M, Codognotto A, Bicego M, Pines A, Tell G, D'Andrea P 2005 Autocrine/paracrine stimulation of purinergic receptors in osteoblasts: Contribution of vesicular

ATP release. Biochem Biophys Res Commun **331:**1429–1438.
20. Nakano Y, Addison WN, Kaartinen MT 2007 ATP-mediated mineralization of MC3T3-E1 osteoblast cultures. Bone **41:**549–561.
21. Hoebertz A, Arnett TR, Burnstock G 2003 Regulation of bone resorption and formation by purines and pyrimidines. Trends Pharmacol Sci **24:**290–297.
22. Morrison MS, Turin L, King BF, Burnstock G, Arnett TR 1998 ATP is a potent stimulator of the activation and formation of rodent osteoclasts. J Physiol **511:**495–500.
23. Zimmermann H 2000 Extracellular metabolism of ATP and other nucleotides. Naunyn Schmiedebergs Arch Pharmacol **362:**299–309.
24. Buckley KA, Hipskind RA, Gartland A, Bowler WB, Gallagher JA 2002 Adenosine triphosphate stimulates human osteoclast activity via upregulation of osteoblast-expressed receptor activator of nuclear factor-kappa B ligand. Bone **31:**582–590.
25. Wu W, Zhang X, Zanello LP 2007 1α,25$(OH)_2$-vitamin D_3 antiproliferative actions involve vitamin D receptor-mediated activation of MAPK pathways and AP-1/p21(waf1) upregulation in human osteosarcoma. Cancer Lett **254:**75–86.
26. Gosling M, Smith JW, Poyner DR 1995 Characterization of a volume-sensitive chloride current in rat osteoblast-like (ROS 17/2.8) cells. J Physiol **485:**671–682.
27. Mizwicki MT, Keidel D, Bula CM, Bishop JE, Zanello LP, Wurtz JM, Moras D, Norman AW 2004 Identification of an alternative ligand-binding pocket in the nuclear vitamin D receptor and its functional importance in 1α,25$(OH)_2$-vitamin D_3 signaling. Proc Natl Acad Sci USA **101:**12876–12881.
28. Knight GE, Bodin P, De Groat WC, Burnstock G 2002 ATP is released from guinea pig ureter epithelium on distension. Am J Physiol Renal Physiol **282:**F281–F288.
29. Zhang X, Zanello LP 2008 Vitamin D receptor-dependent 1α,25$(OH)_2$-vitamin D_3-induced antiapoptotic PI3K/Akt signaling in osteoblasts. J Bone Miner Res **23:**1238–1248.
30. Barg S 2003 Mechanisms of exocytosis in insulin-secreting B-cells and glucagon-secreting A-cells. Pharmacol Toxicol **92:**3–13.
31. Becherer U, Moser T, Stuhmer W, Oheim M 2003 Calcium regulates exocytosis at the level of single vesicles. Nat Neurosci **6:**846–853.
32. Levitan ES 2008 Signaling for vesicle mobilization and synaptic plasticity. Mol Neurobiol **37:**39–43.
33. Meszaros JG, Karin NJ, Farach-Carson MC 1996 Voltage-sensitive calcium channels in osteoblasts: Mediators of plasma membrane signalling events. Connect Tissue Res **34-5:**161–165.
34. Liu R, Li W, Karin NJ, Bergh JJ, Adler-Storthz K, Farach-Carson MC 2000 Ribozyme ablation demonstrates that the cardiac subtype of the voltage-sensitive calcium channel is the molecular transducer of 1α,25$(OH)_2$-vitamin D_3-stimulated calcium influx in osteoblastic cells. J Biol Chem **275:**8711–8718.
35. Le Mellay V, Grosse B, Lieberherr M 1997 Phospholipase C β and membrane action of calcitriol and estradiol. J Biol Chem **272:**11902–11907.
36. Zhang X, Zanello LP 2005 Activation of the PI3K/Akt(PKB)/Bad cascade by 1α,25$(OH)_2$-vitamin D_3 in osteoblasts. Mol Biol Cell **16:**B522.
37. Barg S, Huang P, Eliasson L, Nelson DJ, Obermüller S, Rorsman P, Thévenod F, Renström E 2001 Priming of insulin granules for exocytosis by granular Cl^- uptake and acidification. J Cell Sci **114:**2145–2154.
38. Thevenod F 2002 Ion channels in secretory granules of the pancreas and their role in exocytosis and release of secretory proteins. Am J Physiol Cell Physiol **283:**C651–C672.
39. Zanello LP, Norman AW 1996 1α,25$(OH)_2$ vitamin D_3-mediated stimulation of outward anionic currents in osteoblast-like ROS 17/2.8 cells. Biochem Biophys Res Commun **225:**551–556.
40. Biswas P, Zanello LP 2005 Calcium signals associated with 1α,25$(OH)_2$ vitamin D_3–regulated exocytosis in osteoblasts. Mol Biol Cell **16:**B428.
41. Vertino AM, Bula CM, Chen JR, Almeida M, Han L, Bellido T, Kousteni S, Norman AW, Manolagas SC 2005 Nongenotropic, anti-apoptotic signaling of 1α,25$(OH)_2$ vitamin D_3 and analogs through the ligand binding domain of the vitamin D receptor in osteoblasts and osteocytes. Mediation by Src, phosphatidylinositol 3-, and JNK kinases. J Biol Chem **280:**14130–14137.
42. Orriss IR, Utting JC, Brandao-Burch A, Colston K, Grubb BR, Burnstock G, Arnett TR 2007 Extracellular nucleotides block bone mineralization in vitro: Evidence for dual inhibitory mechanisms involving both P2Y2 receptors and pyrophosphate. Endocrinology **148:**4208–4216.

Received in original form July 31, 2008; revised form December 3, 2008; accepted March 11, 2009.